Journal of The Electrochemical Society, **153** (8) C562-C566 (2006)
0013-4651/2006/153(8)/C562/5/$20.00 © The Electrochemical Society

Single-Source Chemical Vapor Deposition of SiC Films in a Large-Scale Low-Pressure CVD Growth, Chemical, and Mechanical Characterization Reactor

Christopher S. Roper,[a] Velimir Radmilovic,[b] Roger T. Howe,[c] and Roya Maboudian[a,z]

[a]*Berkeley Sensor and Actuator Center, Department of Chemical Engineering, University of California, Berkeley, California, USA*
[b]*National Center for Electron Microscopy, Lawrence Berkeley National Laboratory, Berkeley, California, USA*
[c]*Department of Electrical Engineering, Stanford University, Stanford, California, USA*

The development and characterization of a silicon carbide (SiC) deposition process from a single source precursor, 1,3-disilabutane, in a large-scale reactor is described. Deposition was performed simultaneously on fifteen, 4 in. Si wafers in a 4 or 6 in. wafer-capable horizontal low-pressure chemical vapor deposition reactor. Amorphous SiC is obtained at temperatures of 750°C and below, while some polycrystallinity is obtained at temperatures of 800°C and above. Highly uniform and relatively smooth films are realized using a closed wafer boat. A maximum growth rate of 0.45 μm/h is attained at 750°C. Residual stress in the film is characterized and found to be greater than 1.3 GPa (tensile) across a wide range of deposition temperatures. Stress profiling is performed to investigate the stress distribution throughout the films. Microfabrication on the wafer level using SiC as a structural layer is also demonstrated.
 [DOI: 10.1149/1.2208911]

Manuscript submitted March 2, 2006; revised manuscript received April 3, 2006. Available electronically June 13, 2006.

Silicon carbide has recently been pursued as both a microelectromechanical systems (MEMS) structural material for use in harsh environments[1,2] as well as a MEMS antistiction and wear-reducing coating.[3,4] Chemical vapor deposition (CVD) of SiC has been performed using a variety of precursors and sundry deposition conditions.[5-9] One such precursor is 1,3-disilabutane ($CH_3SiH_2CH_2SiH_3$) (DSB), a single-source precursor which allows the growth of polycrystalline 3C–SiC thin films at relatively low deposition temperatures.[10] Deposition of SiC using DSB has been reported on 2 in. diameter silicon wafers in a low-pressure CVD (LPCVD) reactor. For SiC to become a standard MEMS material, not only must it be deposited in a well-controlled and characterized process, but it must also be deposited onto substrates compatible with other MEMS processing steps. Such substrates are currently 4 and 6 in. wafers.

One of the desirable qualities of CVD film growth is uniformity. High cross-wafer uniformity and high cross-load uniformity are both important to assure uniformity between all final MEMS devices made from these films. LPCVD is often selected over atmospheric pressure CVD because the large diffusion coefficients at lower pressures tend to lead to more uniform films; however, in certain LPCVD thin-film deposition processes, including deposition of doped polycrystalline silicon (poly-Si) and low-temperature silicon oxide (LTO), cross-wafer uniformity can be poor. The cause of poor cross-wafer uniformity has been traced to radial depletion of reactive intermediates formed through homogeneous gas-phase reactions. In these cases cross-wafer uniformity can be enhanced by using a cage or a closed boat.[11] The closed-boat configuration is known to increase the surface area near the edges of the wafers such that the reactive intermediates deposit preferentially on the boat. Film growth on the wafers is then limited mainly to a heterogeneous surface decomposition reaction. This leads to increased uniformity at the cost of lower overall growth rate.[11]

Residual stress is important in film growth.[12] Films with nonzero average residual film stress cause the film–substrate composite to curve. In addition, thin films with nonzero stress expand or contract when released from underlying layers, depending on whether the stress is compressive or tensile. Alteration of geometry upon release and cracking both make high stress levels undesirable for micromachining. Low stress gradients are also desirable as structures fabricated from films with large stress gradients either curl upward or downward when released, depending on whether the gradient is positive or negative.

This paper reports the deposition and characterization of poly-SiC thin films with thicknesses ranging from 75 nm to 3.5 μm in a LPCVD reactor from DSB on 4 in. diam Si wafers, which are compatible with equipment in most present-day MEMS microfabrication facilities. We have explored the effect of deposition temperature on growth rate, film stress, stress gradient, and crystallinity. The effect of boat geometry on uniformity, growth rate, and film morphology is also investigated. This is the first known work reporting poly-SiC LPCVD from DSB on 4 in. Si wafers in a closed-boat configuration.

Experimental

Reactor details and deposition parameters.— The SiC films in this work are deposited in a commercial LPCVD Tystar Titan II furnace with a 90 cm hot zone (Fig. 1). A thermocouple inserted into a reactor cantilever indicates that temperature varies by at most 2°C

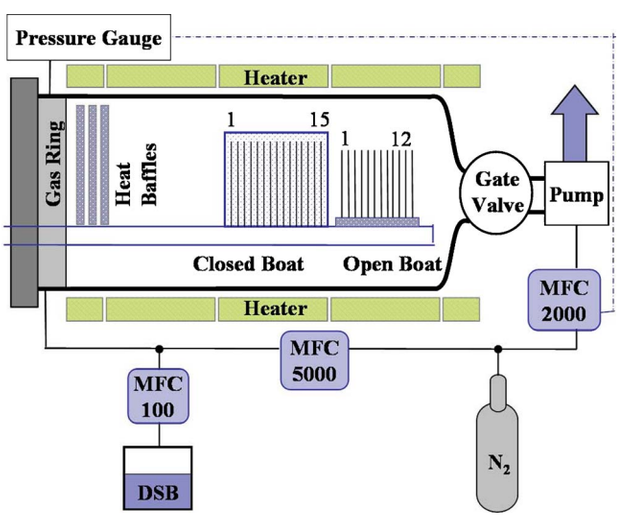

Figure 1. Schematic of Tystar15 LPCVD reactor.

[z] E-mail: maboudin@berkeley.edu

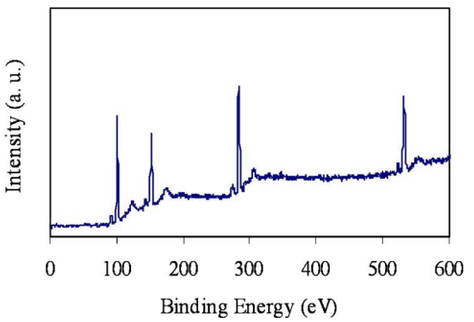

Figure 2. XPS spectrum of SiC deposited at 800°C.

in the reactor hot zone. The Tystar furnace has a base pressure of 2 mTorr achieved with an Edwards QMB500 roots blower in conjunction with an Edwards QDP40 mechanical pump. The tube diameter allows film deposition onto either 4 or 6 in. diam wafers, with orientation perpendicular to the gas stream. For the experiments reported in this work, the hot zone temperature is varied between 700 and 850°C. The deposition pressure is set at 150 mTorr. The precursor, DSB (JSI Silicone, 98% purity), is further purified with freeze–pump–thaw cycles using liquid nitrogen before being installed in the reactor. The DSB flows at a rate of 45 sccm, controlled by a Tylan 2900 Series mass flow controller. The deposition is carried out for 60 min when depositing at either 800 or 850°C. This time is reduced to 30 min for depositions at 700 or 750°C to avoid film cracking, which occurs at larger thicknesses under these conditions. Experiments are conducted with open and closed borofloat glass boats (Angle Slotted Quartz, Inc.). The open boat holds 12 wafers with an interwafer spacing of 0.9 cm. The closed boat consists of a cylinder which surrounds the wafers with slits in the cylinder to allow reactant gas to reach the wafers and holds 15 wafers with an interwafer spacing of 1.2 cm.

Sample preparation.— All films are grown on 4 in. diam p-type Si(100) wafers with resistivity of 1–50 Ω cm. Prior to deposition, wafers are cleaned by a 10 min piranha clean (83% sulfuric acid and 17% hydrogen peroxide at 120°C), rinsed in deionized water (18 MΩ cm), and dried. The final resistivity of the rinsing water is greater than 16 MΩ cm.

To demonstrate that silicon carbide can be deposited on oxide surfaces as well as bare silicon, a silicon oxide layer is grown on some of the silicon wafers. To create these substrates, 4 in. diam p-type Si(100) test wafers are cleaned as above. These wafers are thermally oxidized for 40 min in water vapor at 1100°C. This leads to a 0.5 μm layer of silicon oxide on the surface of the wafer. Prior to SiC deposition the wafers are cleaned again as described above.

Characterization techniques.— Atomic composition of the films was examined with X-ray photoelectron spectroscopy (XPS). The system used is an Omicron Dar400 achromatic Mg K X-ray source (15 keV, 20 mA emission current) and an Omicron EA125 hemispherical analyzer operated in constant energy analyzer mode with 50 eV pass energy. Dynamic secondary ion mass spectrometry (SIMS) is performed using a Physical Electronics 6650 Quadrupole SIMS with Cs^+ ions to measure the oxygen impurity profile in the SiC films. Grazing incidence X-ray diffraction (XRD) using a Philips diffractometer with an incident angle of 1° is used to identify the crystal orientation of the thin films. The crystal structure of the films is determined by transmission electron microscopy (TEM) in a JEOL 200CX electron microscope using bright field (BF) and dark field (DF) imaging and selected area diffraction (SAD) techniques. Samples less than 10 μm thick containing cross sections of SiC films are prepared for TEM using a series of mechanical grinding, dimpling, and polishing steps. Samples are then ion milled in a Fishione ion mill at an angle of 6°. The thickness of the films is determined by optical reflectometry with a NanoSpec model 3000 thickness measurement system[10] with a 25 μm diam beam spot. Atomic force microscopy (AFM) using a Digital Instruments Multimode Nanoscope IIIa operated in contact mode is used to measure surface roughness.

The method of measuring the stress variation throughout the SiC thin films is that used by Krulevitch et al. on poly-Si thin films in which thin layers of the film are successively etched away and radius of curvature measurements are made after each step.[12] Average residual film stress is calculated using a modified Stoney equation

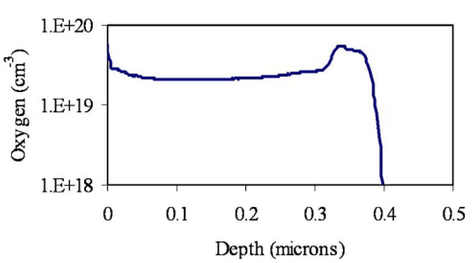

Figure 3. SIMS oxygen impurity profile for film deposited at 800°C.

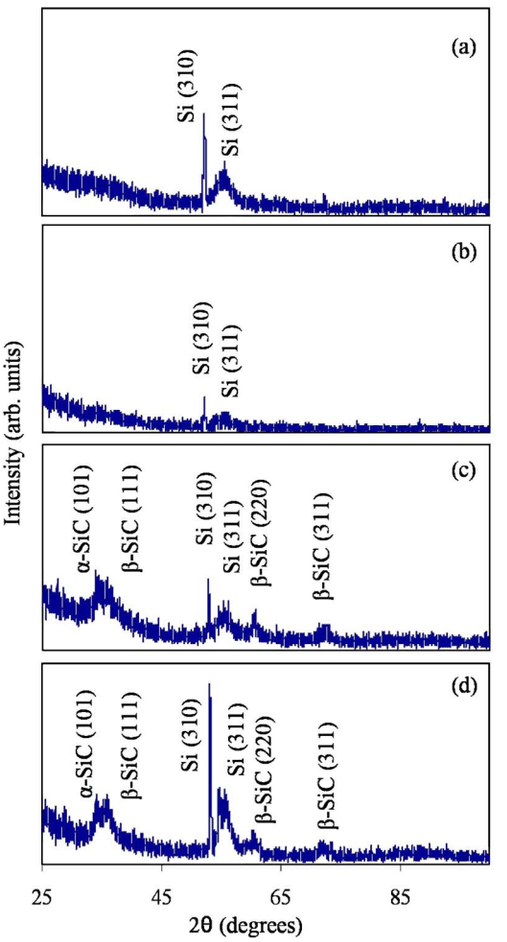

Figure 4. Thin-film XRD spectra of SiC films deposited at (a) 700, (b) 750, (c) 800, and (d) 850°C.

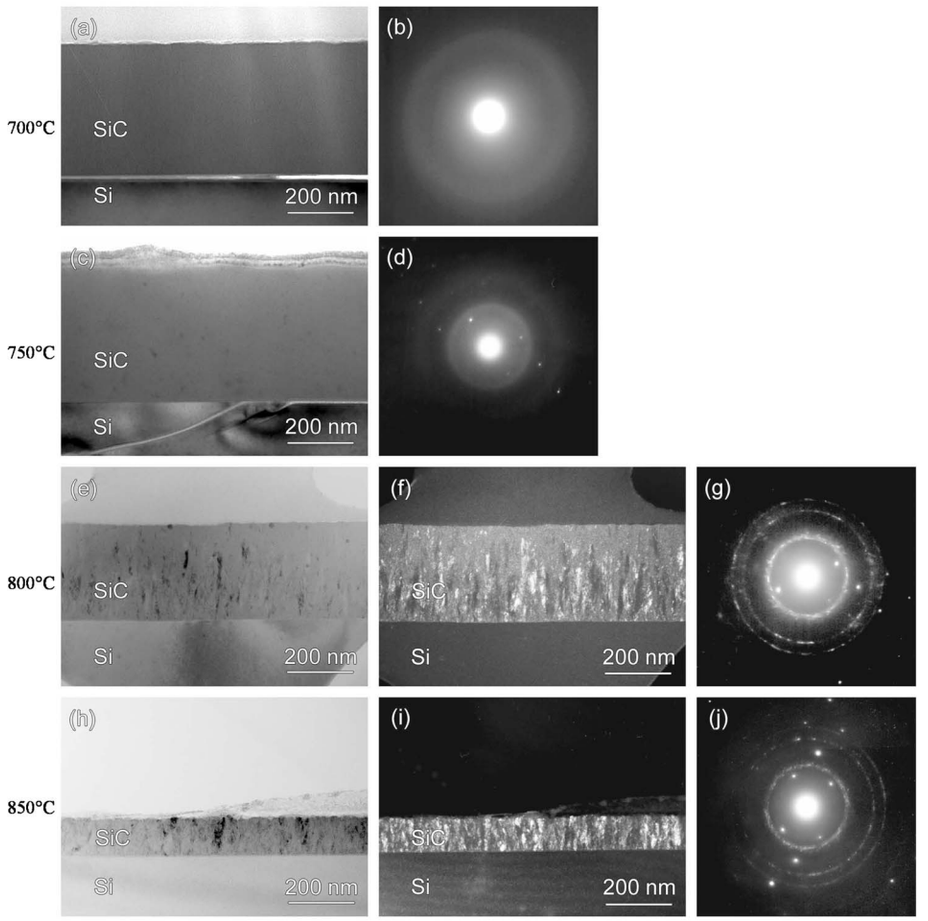

Figure 5. TEM images for SiC films deposited at 700°C: (a) BF image and (b) SAD pattern; 750°C: (c) BF image and (d) SAD pattern; 800°C: (e) BF image, (f) DF image, and (g) SAD pattern; and 850°C: (h) BF image, (i) DF image, and (j) SAD pattern.

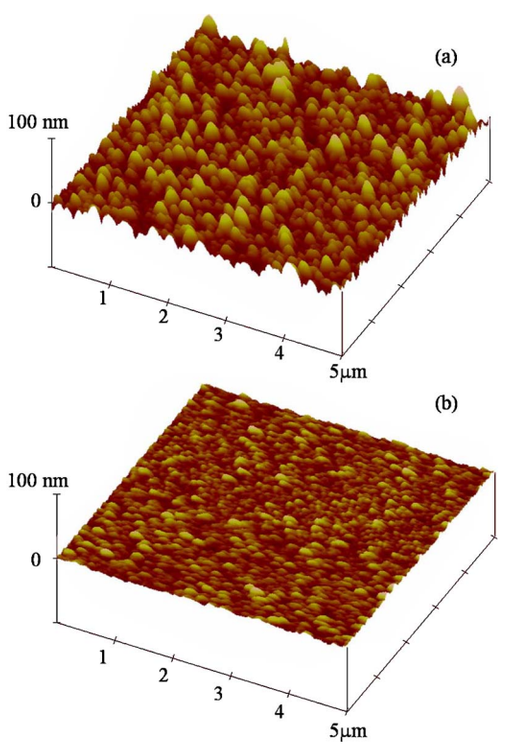

Figure 6. AFM images (5 × 5 m area, 100 nm z-scale) of films deposited in (a) open boat (film thickness 0.7 μm) and (b) closed boat (film thickness 0.3 μm).

$$\sigma = E_s t_s^2 [6 t_f (1 - \upsilon_s)]^{-1} (\rho_2^{-1} - \rho_1^{-1}) \quad [1]$$

The substrate thickness, t_s, is determined using a micrometer. The film thickness, t_f, is determined using reflectometry as described above. The wafer curvatures with and without the deposited thin film, ρ_2 and ρ_1, respectively, are determined using a Tencor FLX-2320 (Flexus) system which measures vertical displacement with a laser interferometer and fits a radius of curvature to the measured profile. E_s is the elastic modulus of the substrate and υ_s is the Poisson's ratio of the substrate. The biaxial modulus of the substrate, $E_s/(1 - \upsilon_s)$, is taken to be 180.5 GPa for silicon ⟨100⟩.

Stress profiling using Eq. 1 is performed by successively etching away a layer of the SiC thin film using a HBr- and Cl_2-based transformer coupled plasma (TCP) etch,[13] performing NanoSpec thickness measurements and using the Flexus to measure radius of curvature. To quantify the stress gradient, cantilever beam arrays are fabricated by first growing a LTO layer 2 μm thick on top of a SiC film already deposited on a Si(100) substrate. Photoresist is spun on top of the LTO layer. It is patterned with a GCA 6200 wafer stepper, developed and baked at 120°C for 24 h. The LTO layer is etched using a CF_4- and CHF_3-based plasma. The SiC layer is etched with HBr- and Cl_2-based TCP.[13] The photoresist is striped using J. T. Baker PRS3000 and the LTO is removed using concentrated (49%) HF. The SiC structures are released using a timed isotropic undercut etch with XeF_2.

Results and Discussion

Chemical composition.— Film composition is investigated using XPS. The photoelectron spectra of films deposited in the reactor exhibit only silicon, carbon, and oxygen peaks. Figure 2 depicts a

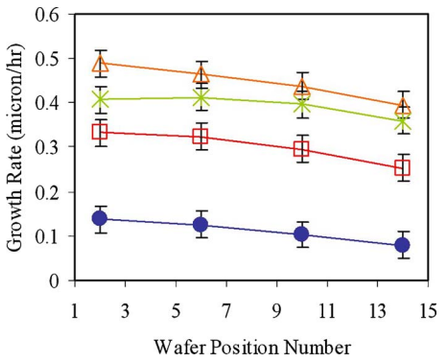

Figure 7. Growth rate in closed-boat geometry as function of wafer position for various deposition temperatures: (•) 850, (□) 800, (△) 750, and (X) 700°C.

spectrum for a film deposited at 800°C. Referencing the portion of the C(1s) peak due to ex situ adsorbed hydrocarbon contaminants and codeposited carbon to 285.0 eV binding energy, the peaks for Si (2p) and C (1s) due to SiC are found at 101.5 and 282.4 eV binding energies, respectively; these are consistent with previous work on LPCVD SiC.[10] The C (1s) and Si (2p) peak areas indicate the presence of stoichiometric SiC at the surface of the films. Brief sputtering with 2.0 keV Ar^+ ions significantly reduces the intensity of O (1s) peak, indicating that most of the oxygen is due to adsorbed surface species; however, the presence of such species prevents accurate determination of oxygen content in the films from the O (1s) peak. SIMS is utilized to measure the oxygen impurity profile in the films and is found to be 2×10^{19} cm^{-3}, typical of horizontal LPCVD reactors.[14] Figure 3 depicts SIMS data for a film deposited at 800°C. SIMS analysis also indicates that the film is carbon-rich, in contrast to XPS results.

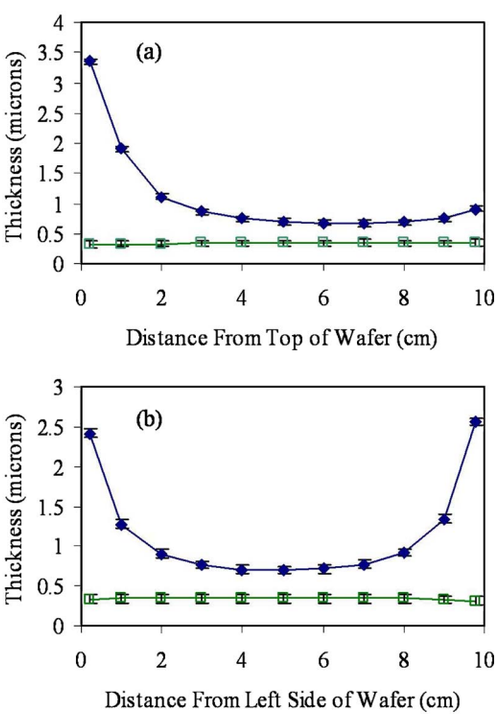

Figure 8. (a) Wafer no. 3 vertical thickness profiles for (♦) open boat and (□) closed boat configurations. (b) Wafer no. 3 horizontal thickness profiles for (♦) open boat and (□) closed boat configurations.

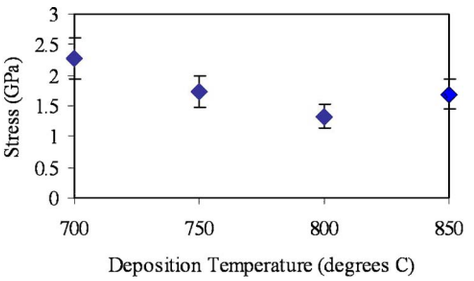

Figure 9. Average film stress as a function of deposition temperature.

Crystallinity and film morphology.— Thin-film XRD is used to determine the crystallinity of the films. At both 800 and 850°C, α-SiC(101), β-SiC(111), β-SiC(220), and β-SiC(311) peaks are observed (Fig. 4). This indicates that films deposited at 800°C and above have polycrystalline structure. At 750°C and below the films appear completely amorphous. TEM images along with corresponding diffraction patterns for films deposited at 700, 750, 800, and 850°C are depicted in Fig. 5. Figure 5a and c shows the BF images of fully amorphous films deposited at 700 and 750°C, respectively. The fully amorphous nature is clearly indicated by the halos present in the diffraction patterns (Fig. 5b and d). The spots in Fig. 5d are due to the silicon substrate. Similar spots are not observed in Fig. 5b because the region of the film selected for SAD delaminated from the Si substrate during sample preparation. Figure 5e and f depicts the BF and DF images of the film deposited at 800°C. The corresponding SAD pattern is shown in Fig. 5g. It is apparent from the ring pattern that the SiC deposited at 800°C is polycrystalline, but some amount of amorphous material may still be present. Figure 5h and i shows the BF and DF images of the film deposited at 850°C. The corresponding SAD pattern shown in Fig. 5j indicates the polycrystalline nature of the film. From Fig. 5e-i, the shape of the SiC grains is seen to be columnar. Based on Si spot pattern as an internal standard calibration, the ring radii are used to index the SAD patterns in Fig. 5g and j. The most prominent rings are due to the β-SiC(111), β-SiC(220), and β-SiC(311) planes. This is consistent with the peaks found with XRD. Based on these analyses, it can be concluded that the minimum temperature that provides a polycrystalline film without amorphous regions is 850°C.

The surface roughness is measured for the deposited films using AFM. The AFM images obtained for films deposited at 800°C are depicted in Fig. 6. The root–mean–square (rms) roughness of a 0.7 μm thick open-boat film is 6.8 nm, while the rms roughness of the closed-boat film is 1.6 nm at a film thickness of 0.3 μm.

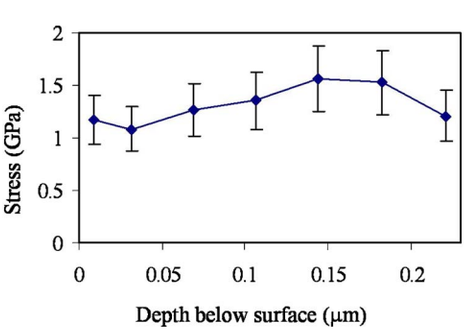

Figure 10. Stress profile for SiC film deposited at 800°C.

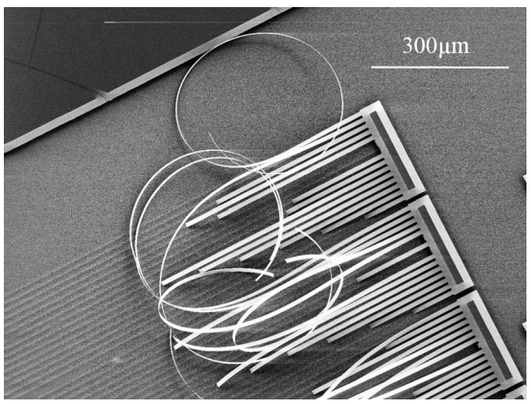

Figure 11. Microfabricated cantilever beam array using 300 nm thick SiC films deposited at 800°C.

Growth rate and uniformity.— The growth rates at varying deposition temperatures are examined. Figure 7 shows the average growth rate on wafers located at different axial positions in the closed boat. Growth rate is observed to decrease toward the reactor exit, which is located beyond wafer no. 15, indicating that the precursor is being depleted down the length of the reactor. Additionally, growth rate decreases as temperature increases above 750°C. This may be explained by the following. The reaction rates for the decomposition of both DSB and $CH_3SiH_2CH_2SiH$ increase with increasing temperature; however, as temperature increases, the reaction pathway involving the $CH_3SiH_2CH_2SiH$ radical, which preferentially reacts on the walls of the closed boat, becomes more kinetically favorable as reported by Valente et al..[15] With increasing temperature, reaction rate increases, but after a point so much of the precursor is consumed through SiC deposition on the closed-boat walls that the net effect is a decrease in average wafer growth rate. A finite element model is under development to verify this explanation.

Cross-wafer thickness uniformity is examined for the open and closed boats. Figure 8 shows the results for deposition at 800°C, indicating that the films deposited in the closed-boat geometry have greater uniformity than those deposited using the open boat, similar to other LPCVD processes.[11]

Kinetic and quantum chemical modeling by Valente et al.,[15] which has been used to accurately predict SiC LPCVD growth from DSB, predicts two dominant pathways for the formation of SiC. The first pathway consists of a heterogeneous surface decomposition of DSB to SiC and H_2. The second pathway entails a homogenous decomposition of DSB to $CH_3SiH_2CH_2SiH$ and the subsequent surface decomposition of $CH_3SiH_2CH_2SiH$ to SiC and H_2. The sticking coefficient of $CH_3SiH_2CH_2SiH$ is near unity, 2 to 3 orders of magnitude higher than that of DSB. We postulate that the predominant reactive intermediate, $CH_3SiH_2CH_2SiH$, is depleted radially in the open boat, leading to highly nonuniform film deposition; however, it reacts on the boat walls in the closed-boat configuration and does not contribute significantly to the growth of SiC on the wafers in such a configuration. This also explains the asymmetry in the open-boat vertical-thickness profile (Fig. 8a). The open boat and cantilevers increase the surface area only at the bottom edges on the wafers; thus, the thickness variation is lower near the bottom of the wafers.

Film average stress and strain gradient.— The effect on average film stress of deposition temperature (Fig. 9) is investigated. All average stresses are over 1.3 GPa tensile, much higher than in other SiC films deposited by LPCVD from DSB.[16] TEM observations indicate that film microstructure is not similar to findings in previous works in which a columnar growth was observed at growth rates 10 times greater than those reported in this work. Work is underway to reduce the residual stress.

The stress profiles of SiC films deposited at 700 to 850°C are investigated. A characteristic profile is presented in Fig. 10. For each stress profiling measurement, the average stress of the entire film as calculated from a single interferometry measurement is compared to the average stress as calculated from the average of all the individual layer stress measurements. These two figures differ by less than 5% for each condition. In most cases, the stress is found to increase near the substrate–film interface to a maximum value and then slowly decay with further increasing thickness. This behavior is consistent with stress profiles for thin films of high-melting-point materials.[17] In all cases there is change in stress with thickness which results in curled cantilevers. An example is shown in Fig. 11, with beams fabricated from a film deposited at 800°C, curling down, indicating a negative strain gradient, which is consistent with Fig. 10.

Conclusions

A large-scale SiC LPCVD process utilizing DSB single precursor has been demonstrated and characterized. Current advantages of this system over other existing systems include the ability to deposit on 4 and 6 in. wafers, high cross-wafer uniformity, and low surface roughness. As-deposited film stress is over 1.3 GPa, which limits the MEMS applications for this film to thin-film coatings.

Acknowledgments

The authors gratefully acknowledge DARPA MTO for funding this work. One author (C.S.R.) acknowledges the partial support of a NSF graduate student fellowship. The authors also acknowledge Luca Magagnin of the Politecnico di Milano for assistance with the thin-film XRD, Tom Mates of the University of California, Santa Barbara, for the SIMS analysis, as well as William Flounders and Robert Hamilton of the UC Berkeley Microfabrication Lab. This work is supported by the Director, Office of Science, Office of Basic Energy Sciences, Materials Sciences, and Engineering Division of the U.S. Department of Energy under contract no. DE-AC02-05CH1123.

University of California of Berkeley assisted in meeting the publication costs of this article.

References

1. M. Mehregany, C. A. Zorman, S. Roy, A. J. Fleischman, C. H. Wu, and N. Rajan, *Int. Mater. Rev.*, **45**, 85 (2000).
2. C. R. Stoldt, C. Carraro, W. R. Ashurst, D. Gao, R. T. Howe, and R. Maboudian, *Sens. Actuators, A*, **97-8**, 410 (2002).
3. N. Rajan, M. Mehregany, C. A. Zorman, S. Stefanescu, and T. P. Kicher, *J. Microelectromech. Syst.*, **8**, 251 (1999).
4. W. R. Ashurst, M. B. J. Wijesundara, C. Carraro, and R. Maboudian, *Tribol. Lett.*, **17**, 195 (2004).
5. S. Nishino, J. A. Powell, and H. A. Will, *Appl. Phys. Lett.*, **42**, 460 (1983).
6. J. H. Boo, K. S. Yu, Y. Kim, S. H. Yeon, and I. N. Jung, *Chem. Mater.*, **7**, 694 (1995).
7. J. H. Boo, S. B. Lee, K. W. Lee, K. S. Yu, Y. Kim, S. H. Yeon, and I. N. Jung, *J. Vac. Sci. Technol. A*, **19**, 1887 (2001).
8. X. A. Fu, J. L. Dunning, C. A. Zorman, and M. Mehregany, *Sens. Actuators, A*, **119**, 169 (2005).
9. C. A. Zorman, S. Rajgopal, X. A. Fu, R. Jezeski, J. Melzak, and M. Mehregany, *Electrochem. Solid-State Lett.*, **5**, G99 (2002).
10. M. B. J. Wijesundara, G. Valente, W. R. Ashurst, R. T. Howe, A. P. Pisano, C. Carraro, and R. Maboudian, *J. Electrochem. Soc.*, **151**, C210 (2004).
11. A. Yeckel and S. Middleman, *J. Electrochem. Soc.*, **137**, 207 (1990).
12. P. A. Krulevitch, in *Mechanical Engineering*, p. 231, University of California, Berkeley, CA (1994).
13. D. Gao, R. T. Howe, and R. Maboudian, *Appl. Phys. Lett.*, **82**, 1742 (2003).
14. T. I. Kamins and J. E. Turner, *Solid State Technol.*, **33**, 80 (1990).
15. G. Valente, M. B. J. Wijesundara, R. Maboudian, and C. Carraro, *J. Electrochem. Soc.*, **151**, C215 (2004).
16. D. Gao, M. B. J. Wijesundara, and C. Carraro, *J. Microlithogr, Microfabr., Microsyst.*, **2**, 259 (2003).
17. L. B. Freund and S. Suresh, *Thin Film Materials: Stress, Defect Formation, and Surface Evolution*, Cambridge University Press, Cambridge (2003).